Materials and Design 102 (2016) 276–283

Contents lists available at ScienceDirect

Materials and Design

journal homepage: www.elsevier.com/locate/matdes

Mechanical and thermal properties of ABS/montmorillonite nanocomposites for fused deposition modeling 3D printing

Zixiang Weng [a,c], Jianlei Wang [a,c], T. Senthil [a], Lixin Wu [a,b,*]

[a] Key Laboratory of Design and Assembly of Functional Nanostructures, Fujian Institute of Research on the Structure of Matter, Chinese Academy of Sciences, Fuzhou 350002, China
[b] Fujian Provincial Key Laboratory of Nanomaterials, Fujian Institute of Research on the Structure of Matter, Chinese Academy of Sciences, Fuzhou 350002, China
[c] University of Chinese Academy of Sciences, Beijing 100049, China

ARTICLE INFO

Article history:
Received 25 February 2016
Received in revised form 11 April 2016
Accepted 14 April 2016
Available online 16 April 2016

Keywords:
ABS
Montmorillonite
Fused deposition modeling
Nanocomposites
3D printing
Rapid prototyping

ABSTRACT

Acrylonitrile butadiene styrene (ABS) nanocomposites with organic modified montmorillonite (OMMT) were prepared by melt intercalation. ABS nanocomposite filaments for fused deposition modeling (FDM) 3D printing were produced by a single screw extruder and printed by a commercial FDM 3D printer. The 3D printed samples were evaluated by tensile, flexural, thermal expansion and dynamic mechanical tests. The structure of nanocomposites were analyzed by TEM and low angle XRD. Results showed that the addition of 5 wt% OMMT improved the tensile strength of 3D printed ABS samples by 43% while the tensile strength of injection moulding ABS samples were improved by 28.9%. It was found that the addition of OMMT significantly increased the tensile modulus, flexural strength, flexural modulus and dynamic mechanical storage modulus, and decreased the linear thermal expansion ratio and the weight loss of TGA. These novel ABS nanocomposites with better mechanical and thermal properties can be promising materials used in FDM 3D printing.

1. Introduction

Three-dimensional (3D) printing is one of the most versatile and revolutionary additive manufacturing (AM) techniques to create 3D objects with unique structure and diverse properties [1]. Presently, various techniques such as fused deposition modeling (FDM) [2], stereolithography apparatus (SLA) [3], continuous liquid interface production (CLIP) [4], digital light processing (DLP) [5] and selective laser sintering (SLS) [6] have been developed to form stereoscopic objects with complex architecture. In the late 1980s, S. Scott Crump developed FDM 3D printer and it was commercialized by Stratasys in 1990 [7]. Now, FDM has become the most widely used 3D printing method due to its simple-to-use, low-cost and environment-friendly features and is increasingly used in product development, prototyping and manufacturing processes in a variety of industries, including household appliances, automobile, toys, architecture, medical appliances, aircraft and aerospace.

However, the followings limit the application of FDM 3D printing: the mechanical strength of the FDM printed products are usually worse compared with injection moulding due to their weakness points between the layers [8], and also, the thermoplastic materials tend to shrink during the cooling process, resulting in warp of the printed products [9]. To date, the FDM 3D printing has been studied in the fields of building equipments, materials [10], preparation techniques [11] and numerical simulation [12] and attracted more and more interests.

Usually, thermoplastic materials like ABS [13,14], nylon [7,15], polylactic acid (PLA) [16] and their blends [17] are used for FDM 3D printer. To enhance the mechanical properties of 3D printed thermoplastics, fiber-reinforced composites were used. However, addition of fibers often result in that the composites are susceptible to fracture during extrusion. Special additives may be necessary in the extrusion to help produce continuous and homogeneous filaments [18].

In recent years, the emergence of nanocomposites has attracted great interest amongst researchers. By using small volume fractions of nano-additives, mechanical properties [19,20], heat distortion temperature [21,22] and thermal stability [23,24] of a polymer matrix can be improved. Thereinto, polymer/layered silicate (PLS) nanocomposites showed significant improvement in the properties of polymer matrix. Numerous studies reported the PLS nanocomposites exhibited better mechanical property, including dynamic mechanical [25], tensile [26], and flexural properties [21] than that of polymer matrix. Wang et al. [27] studied the thermal properties of ABS/montmorillonite nanocomposite. They observed that the intercalated-exfoliated structure was obtained and the thermal stability of ABS was improved by only 5 wt% of organ-montmorillonite. Lately, Yeh et al. [28] studied the tensile strength of ABS/organoclay nanocomposites, and found that the tensile strength can be improved 15% by adding 3 wt% of organoclay only.

* Corresponding author at: Key Laboratory of Design and Assembly of Functional Nanostructures, Fujian Institute of Research on the Structure of Matter, Chinese Academy of Sciences, Fuzhou 350002, China.
E-mail address: lxwu@fjirsm.ac.cn (L. Wu).

http://dx.doi.org/10.1016/j.matdes.2016.04.045
0264-1275/

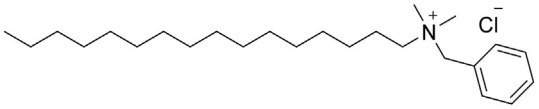

Fig. 1. Chemical structure of HDBAC.

Nowadays, various nanoreinforcements have been used in 3D printed materials, including nanocrystalline cellulose (NCC) [29], SiO_2 [30,31] and layered silicate [32,33]. However, most of them were SLA 3D printed materials. FDM 3D printed nanocomposites have not been fully studied. In this work, FDM 3D printed nanocomposites were prepared. ABS nanocomposite samples were printed by a commercial FDM 3D printer. The mechanical properties of 3D printed nanocomposites samples were evaluated and compared to those of injection moulding samples. The thermal properties of ABS nanocomposites were also studied. It was found that the polymer nanocomposites could be promising high performance FDM 3D printed materials.

2. Experimental

2.1. Materials

The pristine montmorillonite was purchased from Nanocor, trade name as PGW, its CEC is 145 ± 10%meq/100 g. Organic modifier, benzyldimethylhexadecylammonium chloride (HDBAC) was bought from Aladdin Industrial Inc., China. The chemical structure of HDBAC is shown in Fig. 1. ABS pellets, trade name as PA-705, was supplied by Qimei Stock Company, China.

2.2. Modification of pristine clay

According to Pinnavaia's [34,35] method, 10 g of pristine clay was dispersed into 500 mL of distilled water at 60 °C and suspension was obtained. Stoichiometric ratio of HDBAC were added to the suspension and stirred for 5 h. Followed by that, the suspension was cooled at room temperature and then poured into a pressure filtration device. By pressure filtration and washed several times with distilled water until no chloride was detected by 0.1 M AgCl solution, the filter cake was obtained. In order to prevent agglomeration, the filter cake was dried by a freeze drier and fine powder of organic montmorillonite (OMMT) was obtained.

2.3. Preparation of ABS/OMMT nanocomposite

First, ABS pellets and different amount of OMMT powder (1 wt%, 3 wt%, 5 wt% of ABS pellets, denoted by ABS-1, ABS-3 and ABS-5, respectively) were physically mixed by a homogenizer. After that, the mixture of ABS and OMMT were melt mixed using a twin screw extruder (Haake Rheomex OS, Thermo Fisher, Germany). The temperature of 6 heating chambers are 200 °C, 210 °C, 220 °C, 220 °C, 210 °C, 200 °C from funnel to extrusion head respectively. The twin screw extruder used in this study is schematized in Fig. 2. The extrusion speed was 50 rpm. After extrusion, the filament of the ABS/OMMT nanocomposite were cut into pellets with a pelletizer and then they were dried in an oven at 60 °C for 4 h to get rid of moisture.

2.4. Preparation of filament for FDM 3D printer

After desiccation, the pellets of ABS/OMMT nanocomposite were poured into a single screw extruder (SJ-30/25, Zhangjiagang Grand

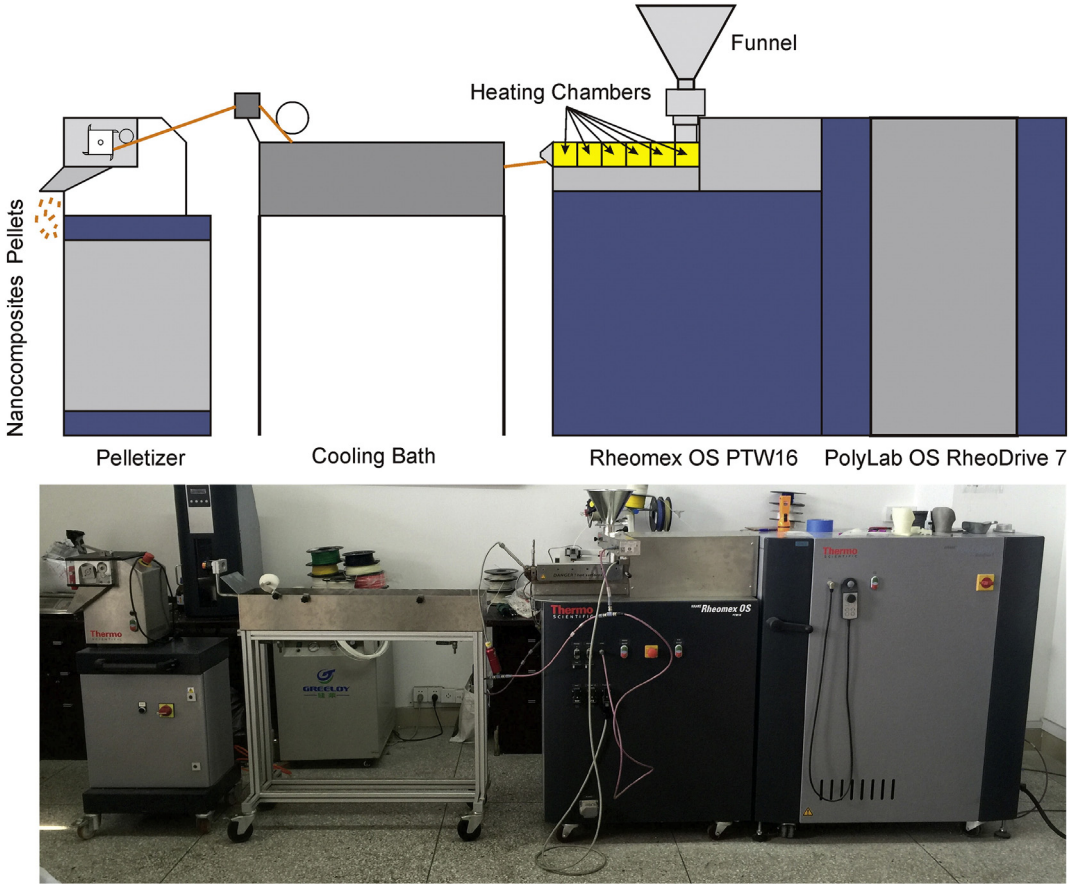

Fig. 2. General view of twin screw extruder.

Fig. 3. General view of single screw extruder used in the production of the ABS/OMMT nanocomposites filament.

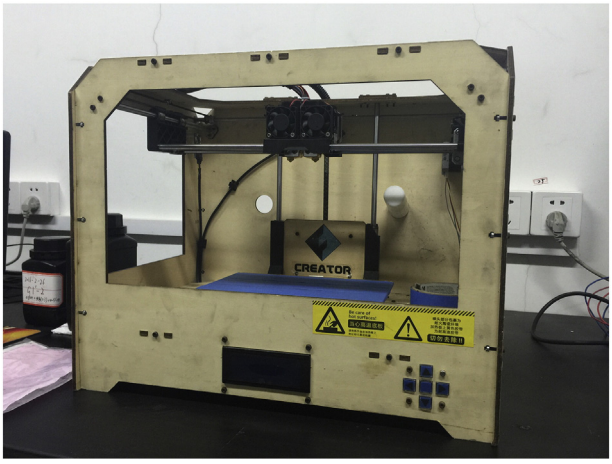

Fig. 4. FDM 3D printer used in this study.

Machinery Co., Ltd., China). The temperature of a two heating chambers was 200 and 210 °C respectively, and the temperature of extrusion head was 190 °C. The rotation speed of the screw is 500 rpm and the diameter of the die is 3 mm. The single screw extruder is shown in Fig. 3. By adjusting the rotating speed of winder, OMMT reinforced ABS nanocomposite filaments with diameter of 1.75 mm ± 0.1 mm were obtained. In order to offset the influence on properties caused by mixing and extrusion, the pure ABS pellets were also remixed by twin screw extruder and single screw extruder.

2.5. Sample preparation

Specimens for mechanical studies of 3D printed samples including tensile strength and flexural strength were designed according to ASTM D790-03 and ASTM D638-03, respectively. Also, the samples used for linear thermo expansion ratio test and DMA test were also made by FDM 3D printer (Creator, Flashforge, China) according to test

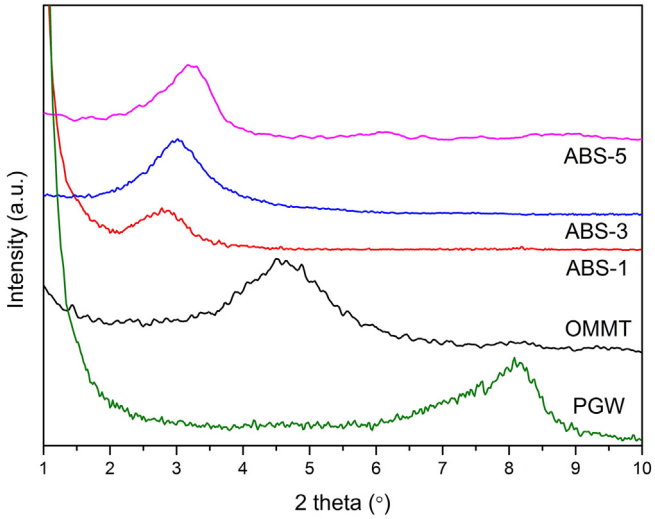

Fig. 5. Low angle X-ray diffraction spectra of ABS/OMMT nanocomposites.

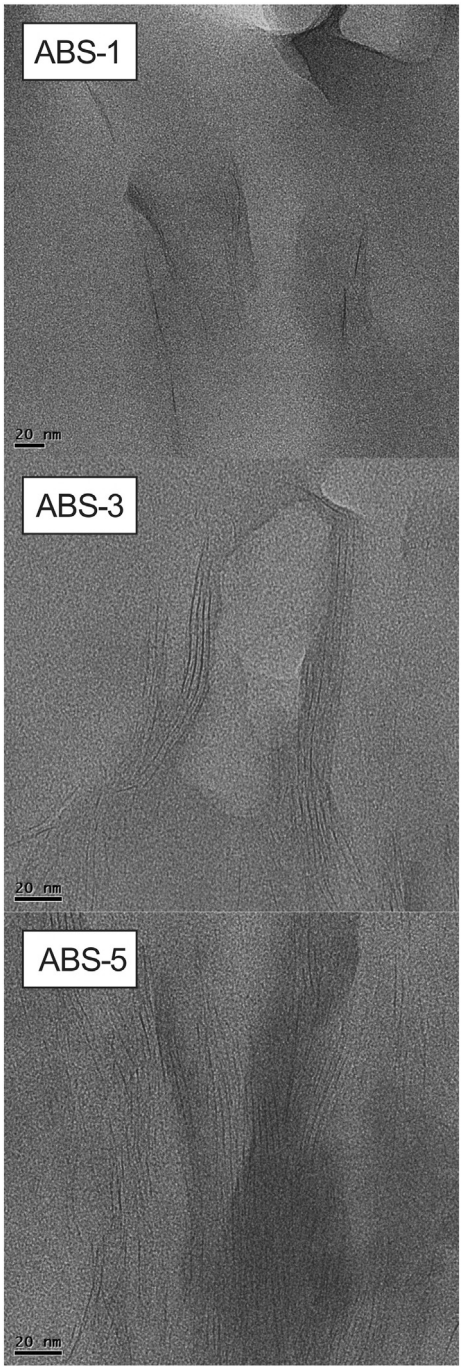

Fig. 6. Transmission electron microscopy micrographs of ABS/OMMT nanocomposites.

Table 1
Mechanical properties of ABS/nanocomposites.

Samples	Tensile strength (injection)	Tensile strength (printed)	Ratio (injection/printed)	Elastic modulus (injection)	Elastic modulus (printed)
Control	49.94	27.59	1.81	1.9	1.2
ABS-1	55.43	31.49	1.76	2.6	1.4
ABS-3	58.63	36.33	1.61	3	2.8
ABS-5	64.36	39.48	1.63	3.2	3.6

requirements. The FDM 3D printer used in this paper was shown in Fig. 4. All the specimens are printed directly on the heating plate without any supports. The filling rate of the specimens were set to 100%, which means that the all specimens are solid structure.

Furthermore, tensile strength specimens using an injection moulding are made by a Haake MiniJet (Thermo Fisher, Germany) to compare the disparity between injection moulding and 3D printing. The temperature of the injection moulding furnace and die was 210 °C and 50 °C, respectively; and the injection pressure was 800 bar.

2.6. Characterization of nanocomposites

X-ray diffraction (XRD) and transmission electron microscope (TEM) were used to examine the microstructure and dispersion morphology of the nanocomposites. The XRD patterns of the samples were obtained using Co Kα radiation (l = 1.78901 Å) in an X'Pert Pro MPD (Philips, Netherlands), diffractometer operating at 40 kV and 30 mA (2θ range from 1° to 10° with a step size of 0.02°). Microstructural characterization of the nanocomposites was carried out using JEM-2010 (JEOL, Japan) at an acceleration voltage of 200 kV. The samples used for TEM were prepared by a cryo-ultramicrotome (EM UC7, Leica, German). Tensile strength and flexural strength of different samples were carried out by a universal material test machine (AGX-100PLUS, Shimadzu, Japan). The strain was obtained by a non-contact extension meter. The analysis speed of the tensile strength and flexural strength was 5 mm/min and 2 mm/min, respectively. The storage modulus of ABS/OMMT nanocomposites was carried out with DMA-Q800 (TA, USA) at a heating rate of 5 °C/min and the test mode was single cantilever. Frequency and amplitude were 1 Hz and 20 μm, respectively. The linear thermo expansion ratio of materials were carried out on a thermal dilatometer (DIL402C, Netzsch, Germany). The initial length of specimens were 25 mm and the analysis temperature range started from 25 to 80 °C. Thermogravimetric analysis was carried out with STA449C (Netzsch, Germany) in the range from 25 to 800 °C under an air atmosphere. The glass-transition temperature was obtained by a differential scanning calorimetry (DSC822e, Mettler-Toledo, Switzerland) in the range of 50 to 160 °C under a nitrogen atmosphere.

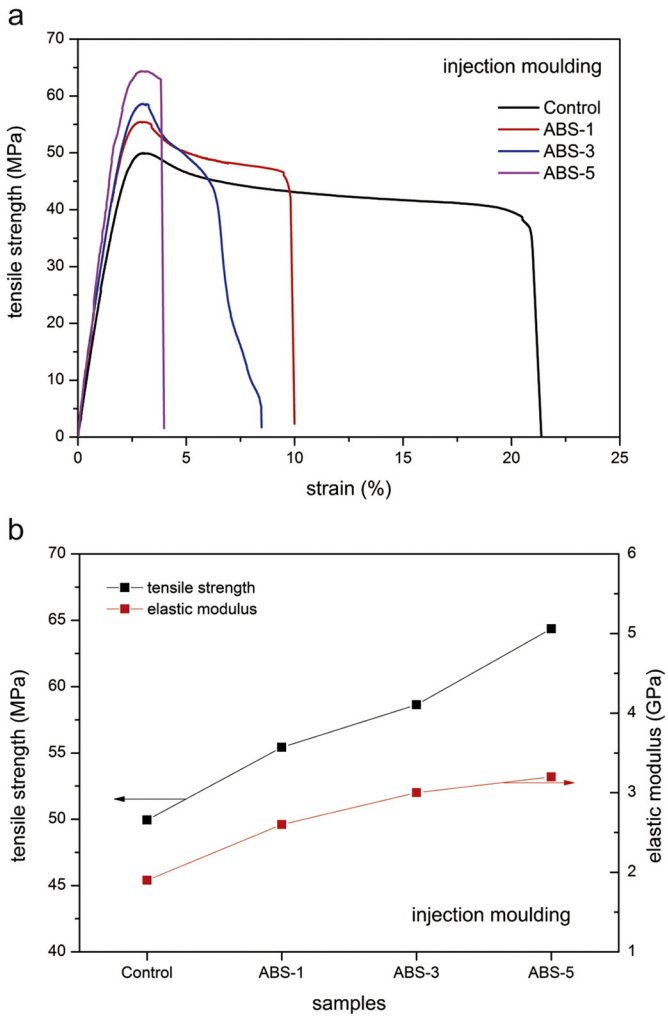

Fig. 7. Tensile strength (a) and elastic modulus (b) of ABS/OMMT nanocomposites samples made by injection moulding.

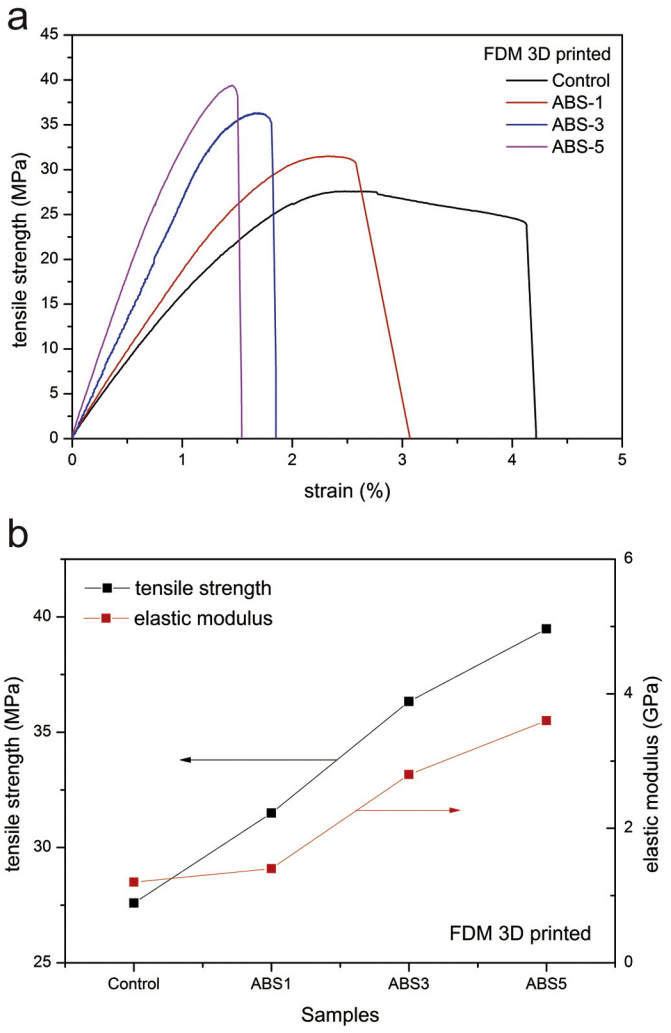

Fig. 8. Tensile strength (a) and elastic modulus (b) of ABS/OMMT nanocomposites samples made by FDM 3D printer.

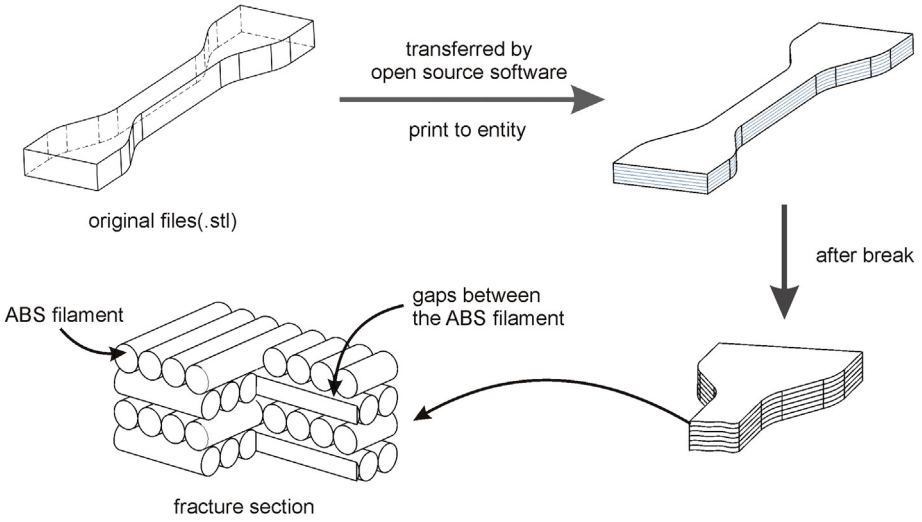

Fig. 9. Illustration of fracture section of printed samples.

3. Results and discussion

3.1. Clay dispersion and morphology

Low angle X-ray diffraction (XRD) was used to determine the microstructure of the clay and its nanocomposites. The XRD patterns of pristine montmorillonite, OMMT and its nanocomposites are shown in Fig. 5. For pristine montmorillonite, a diffraction peak around 8.1° was observed, indicating a *d*-spacing of 1.27 nm. As for OMMT, an obvious diffraction peak at 4.4° was observed, corresponding to a *d*-spacing of 2.3 nm. This observation indicated that the pristine montmorillonite was modified by organic modifier. As expected, the diffraction peak of the nanocomposites was shifted to a lower degree, and the intensity increased with increasing content of the OMMT. The peaks of ABS-1, ABS-3 and ABS-5 were observed at 2.8° (3.7 nm), 3.0° (3.4 nm) and 3.2° (3.2 nm), respectively. This was because some large intercalated tactoids still can be identified in ABS matrix. This similar observation results can be found in numerous literatures [28,36].

The distribution of the clay and morphologies of the nanocomposites were examined by TEM. The representative TEM micrographs of nanocomposites with different amount of montmorillonite are shown in Fig. 6. The dark lines which represents the plate of organoclay were distributed in the ABS matrix and an intercalated structure was formed in the nanocomposites. As evidenced from these image, the interlayer spacing was about 3.5 nm. Even when the clay content increased to 5 wt%, the ABS matrix can also intercalate into the gallery of the montmorillonite. These results were identical to the XRD results. At the same time, the OMMT in the matrix exhibit certain orientation. It can be explained that the montmorillonite was reoriented by the extrusion and winder during the extrusion process.

3.2. Mechanical properties

Tensile strength and elastic modulus of specimens prepared by injection moulding are listed in Table 1 and shown in Fig. 7. Both the tensile strength and the elastic modulus increased substantially with the addition of OMMT content. When the clay loading was 5 wt%, the tensile strength increased from 49.64 MPa (control) to 64.36 MPa and the elastic modulus increased from 1.9 GPa (control) to 3.2 GPa. Simultaneously the elongation at break of different samples decreased with the increase of OMMT loading. It can be explained that the OMMT has much higher modulus and strength than ABS, resulting in higher modulus and strength of ABS/OMMT nanocomposites compared to pure ABS. Moreover, the well-dispersed OMMT can restrict the mobility of ABS molecular chains, resulting in higher stiffness and less elongation of nanocomposites. Similar trend and experimental results were also reported by references [37–39].

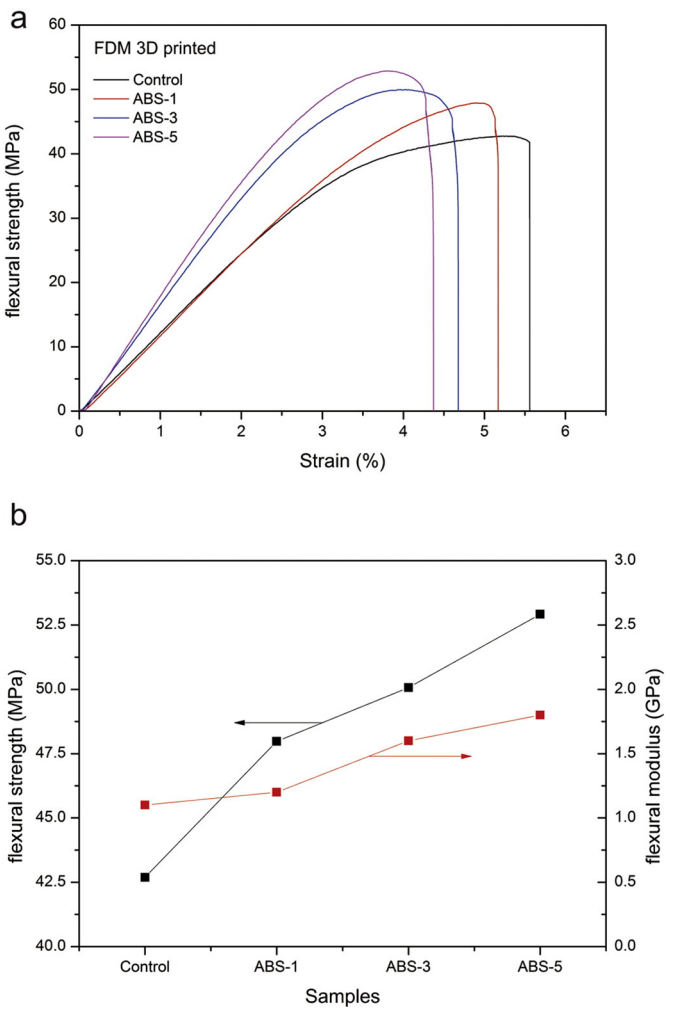

Fig. 10. Flexural strength (a) and flexural modulus (b) of ABS/OMMT nanocomposites samples made by FDM 3D printer.

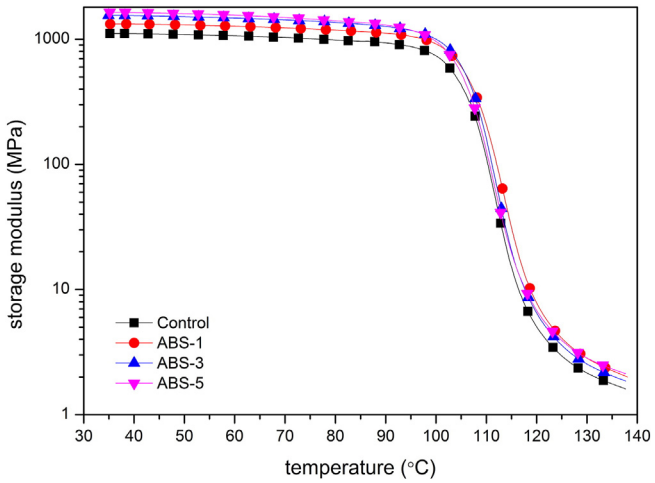

Fig. 11. The curves of storage modulus responses to temperature for the pure ABS and ABS/OMMT nanocomposites.

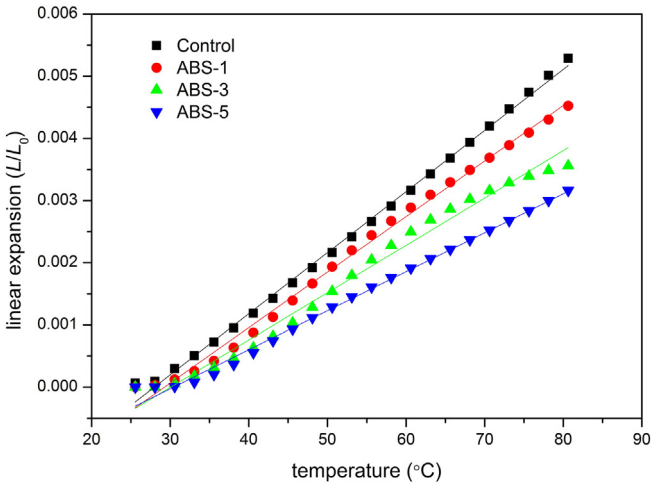

Fig. 13. Thermal expansion coefficient of pure ABS and ABS/OMMT nanocomposites.

Tensile strength and elastic modulus of specimens prepared by 3D printer are listed in Table 1 and shown in Fig. 8. By introducing 5 wt% loading of OMMT, the tensile strength of FDM 3D printed samples increased from 27.59 MPa (control) to 39.48 MPa; the elastic modulus increased from 1.2GPa (control) to 3.6GPa. The ABS/OMMT nanocomposite prepared by using injection moulding method showed higher tensile strength as compared to the FDM printed ones. This is mainly due to 1) during the FDM 3D printing process, the molten filament is attached on the surface of solid layer, resulting in poor entanglement of polymer molecular; 2) as shown in Fig. 9, the arrangement of round and oval filaments in FDM process cannot avoid the gaps between filaments [40], resulting in voids in printed objects, and then reduce the mechanical properties; 3) the high pressure in the injection moulding process can promote the entanglement of polymer chains and increase the density, resulting better mechanical properties. However, by introducing OMMT, the disparity of tensile strength between FDM and injection moulding are narrowed. This positive effect can be contributed by the orientation of OMMT. During the FDM 3D printing, the OMMT were orientated along the direction of extrusion, while the OMMT were randomly arranged during injection moulding. The orientated OMMT have better reinforced effect along the filament direction.

Also, the flexural strength of FDM 3D printed samples were tested and is shown in Fig. 10. Similar to the tensile properties, the flexural strength and flexural modulus increases with increasing content of OMMT. Such phenomenon can also be explained by the toughening effects brought by the OMMT. Fig. 10 illustrates that the increase in flexural strength from 42.69 MPa (control) to 56.92 MPa are achieved at 5 wt% loading of OMMT. These data indicate that OMMT can improve the mechanical properties of ABS as FDM 3D printed materials.

Dynamic mechanical analysis (DMA) was carried out to measure the storage modulus of ABS and its nanocomposites. The storage modulus curves of the pure ABS and ABS nanocomposites are shown in Fig. 11. By incorporation well-dispersed OMMT, a remarkably increased of storage modulus can be achieved with the increase of OMMT loading. At 25 °C, the storage modulus of neat ABS was 1.1 GPa, whereas, beyond 3 wt% of OMMT content (e.g. 5 wt%) resulted in 1.6 GPa increase in the storage modulus. In the glassy state, the storage modulus of organoclay nanocomposites are higher than neat ABS, this indicates that intercalated-exfoliated mixed structure of ABS/organoclay nanocomposites can enhance the mechanical properties of the materials.

3.3. Thermal properties

For FDM 3D printing, the linear expansion ratio of materials is a critical factor to affect the dimension of products. As shown in Fig. 12, for the polymer which has lower linear thermo expansion ratio, the volume of the materials did not change too much with the change of temperature, resulting in less or no warping and deformation of printed samples when cooled to room temperature during FDM 3D printing. On the other hand, neat ABS samples often show warping after FDM 3D printing due to its high linear thermo expansion ratio. When a relative large ABS object is printed by a FDM 3D printer, such shrinkage can lead a delamination between layers leading to a failure of printing. In this study, the linear expansion ratio of neat ABS and ABS/OMMT nanocomposites were examined from room temperature to 80 °C. Fig. 13 and Table 2 show the linear expansion ratio of different samples. It can be seen that the linear thermo expansion ratio decreases with increasing content of OMMT. As reported in Ref [41], the OMMT played as the hard

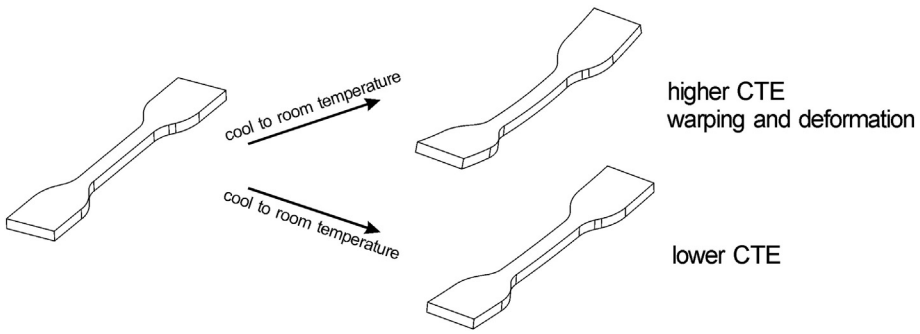

Fig. 12. Illustration of materials warping and deformation in different temperature zone.

Table 2
Linear expansion coefficient of different samples.

Samples	Linear expansion coefficient
Control	9.82×10^{-5} °C^{-1}
ABS-1	8.93×10^{-5} °C^{-1}
ABS-3	7.61×10^{-5} °C^{-1}
ABS-5	6.27×10^{-5} °C^{-1}

segment which can restrict the movement of polymer chain, and lower the linear shrinkage ratio. Therefore, the addition of OMMT in ABS matrix can reduce the warping and deformation of 3D printed objects.

Thermogravimetric analysis (TGA) and differential scanning calorimetry (DSC) was carried out to investigate the effect of OMMT on the thermal behavior of ABS nanocomposites. Fig. 14 shows the typical TGA curves of neat ABS and ABS nanocomposites. Two major stages of weight were observed; The first stage started in the range of 400 °C and ended at about 450 °C, corresponding to the structural decomposition of the polymers. The second stage started around 500 °C and ended at around 600 °C, which indicates that the combustion of residual char. Generally, the introduction of OMMT in polymer matrix enhanced thermal stability by acting as a superior insulator and mass transport barrier to the volatile products generated during decomposition. In this study, the onset of thermal decomposition of ABS/OMMT nanocomposites shifted slightly towards higher temperature range than that of neat ABS, which confirmed the thermal stability brought by OMMT. It can be seen that all the organic moieties disappeared at a temperature of 650 °C, and mainly the inorganic residue remained. Also, with the increase of clay content, the char residue increased.

In addition, the glass transition temperature (T_g) of different samples were investigated by DSC (Fig. 15). According to the DSC results, the T_g value increased with increasing loading of OMMT. This can be explained that the molecular flexibility is limited by the introduction of organoclay. When the organoclay loading increased to 5 wt%, the T_g increased from 99 °C to 112 °C. The results corresponded to the linear expansion ratio results. Therefore, the incorporation of OMMT to ABS matrix have a significant improvement in thermal properties of ABS nanocomposites.

4. Conclusions

A novel ABS/OMMT filaments used for FDM 3D printer were prepared by melt extrusion. First, pristine clay were organic modified by benzyldimethylhexadecylammonium chloride. The low angle XRD the TEM results showed that intercalated structure of ABS/OMMT structure were obtained. Second, different amount of OMMT were mixed with

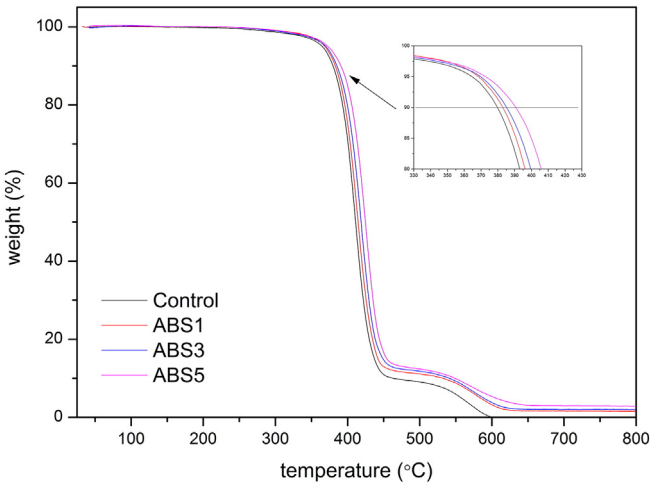

Fig. 14. TGA curves of ABS and ABS/OMMT nanocomposites.

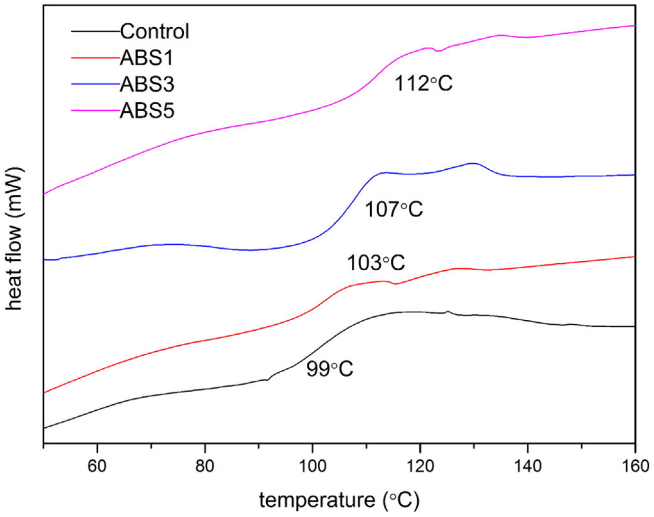

Fig. 15. DSC curves of ABS and ABS/OMMT nanocomposites.

ABS pellets by a twin screw extruder and corresponding filament was prepared by single screw extruder. The tensile strength of ABS/OMMT nanocomposites prepared by FDM 3D printer and injection moulding are both tested. Results showed that the mechanical properties were improved by introducing OMMT into ABS matrix no matter what the manufacture method was. However, OMMT increase the mechanical properties of FDM 3D printed samples more than the increase of mechanical properties for the samples prepared by injection moulding. Also, the linear shrinkage ratio and thermal stability were improved by introducing OMMT.

Acknowledgment

This research was financially supported by the National Natural Science Foundation of China (Grant No.: U1205114), the Natural Science Foundation of Fujian Province (Grant No.: 2014J01217 and 2015H0047), and the “Strategic Priority Research Program” of the Chinese Academy of Sciences (Grant No.: XDA09020301).

References

[1] J.W. Stansbury, M.J. Idacavage, 3D printing with polymers: challenges among expanding options and opportunities, Dent. Mater. Off. Publ. Acad. Dent. Mater. 32 (2016) 54–64.
[2] S.H. Masood, Intelligent rapid prototyping with fused deposition modelling, Rapid Prototyp. J. 2 (1996) 24–33.
[3] M.N. Cooke, J.P. Fisher, D. Dean, C. Rimnac, A.G. Mikos, Use of stereolithography to manufacture critical-sized 3D biodegradable scaffolds for bone ingrowth, J Biomed Mater Res Part B. 64B (2003) 65–69.
[4] J.R. Tumbleston, D. Shirvanyants, N. Ermoshkin, R. Januszewicz, A.R. Johnson, D. Kelly, et al., Continuous liquid interface production of 3D objects, Science 347 (2015) 1349–1352.
[5] I. Cooperstein, M. Layani, S. Magdassi, 3D printing of porous structures by UV-curable O/W emulsion for fabrication of conductive objects, J. Mater. Chem. C 3 (2015) 2040–2044.
[6] M. Agarwala, D. Bourell, J. Beaman, H. Marcus, J. Barlow, Direct selective laser sintering of metals, Rapid Prototyp. J. 1 (1995) 26–36.
[7] S.H. Masood, W.Q. Song, Development of new metal/polymer materials for rapid tooling using fused deposition modelling, Mater. Des. 25 (2004) 587–594.
[8] M. Dawoud, I. Taha, S.J. Ebeid, Mechanical behaviour of ABS: an experimental study using FDM and injection moulding techniques, J. Manuf. Process. 21 (2016) 39–45.
[9] T. Agag, T. Koga, T. Takeichi, Studies on thermal and mechanical properties of polyimide-clay nanocomposites, Polymer 42 (2001) 3399–3408.
[10] D.W. Hutmacher, T. Schantz, I. Zein, K.W. Ng, S.H. Teoh, K.C. Tan, Mechanical properties and cell cultural response of polycaprolactone scaffolds designed and fabricated via fused deposition modeling, J. Biomed. Mater. Res. 55 (2001) 203–216.
[11] S.J. Kalita, S. Bose, H.L. Hosick, A. Bandyopadhyay, Development of controlled porosity polymer-ceramic composite scaffolds via fused deposition modeling, Mater. Sci. Eng. C Biomim. Supramol. Syst. 23 (2003) 611–620.
[12] Y. Zhang, K. Chou, A parametric study of part distortions in fused deposition modelling using three-dimensional finite element analysis, Proc. Inst. Mech. Eng. Part B-J. Eng. Manuf. 222 (2008) 959–967.

[13] S.H. Ahn, M. Montero, D. Odell, S. Roundy, P.K. Wright, Anisotropic material properties of fused deposition modeling ABS, Rapid Prototyp. J. 8 (2002) 248–257.
[14] B.H. Lee, J. Abdullah, Z.A. Khan, Optimization of rapid prototyping parameters for production of flexible ABS object, J. Mater. Process. Technol. 169 (2005) 54–61.
[15] E.J. Pei, J.S. Shen, J. Watling, Direct 3D printing of polymers onto textiles: experimental studies and applications, Rapid Prototyp. J. 21 (2015) 556–571.
[16] D. Drummer, S. Cifuentes-Cuellar, D. Rietzel, Suitability of PLA/TCP for fused deposition modeling, Rapid Prototyp. J. 18 (2012) 500–507.
[17] C.R. Rocha, A.R.T. Perez, D.A. Roberson, C.M. Shemelya, E. MacDonald, R.B. Wicker, Novel ABS-based binary and ternary polymer blends for material extrusion 3D printing, J. Mater. Res. 29 (2014) 1859–1866.
[18] R.W. Gray, D.G. Baird, J.H. Bohn, Effects of processing conditions on short TLCP fiber reinforced FDM parts, Rapid Prototyp. J. 4 (1998) 14–25.
[19] Y. Kojima, A. Usuki, M. Kawasumi, A. Okada, Y. Fukushima, T. Kurauchi, et al., Mechanical-properties of nylon 6-clay hybrid, J. Mater. Res. 8 (1993) 1185–1189.
[20] Y. Kojima, A. Usuki, M. Kawasumi, A. Okada, T. Kurauchi, O. Kamigaito, One-pot synthesis of nylon-6 clay hybrid, J. Poly. Sci. Part A-Polym. Chem. 31 (1993) 1755–1758.
[21] S.S. Ray, K. Yamada, M. Okamoto, K. Ueda, New polylactide-layered silicate nanocomposites. 2. Concurrent improvements of material properties, biodegradability and melt rheology, Polymer 44 (2003) 857–866.
[22] Y. Kojima, A. Usuki, M. Kawasumi, A. Okada, T. Kurauchi, O. Kamigaito, Synthesis of nylon-6-clay hybrid by montmorillonite intercalated with epsilon-caprolactam, J. Polym. Sci. Part A-Polym. Chem. 31 (1993) 983–986.
[23] M. Zanetti, G. Camino, R. Thomann, R. Mullhaupt, Synthesis and thermal behaviour of layered silicate-EVA nanocomposites, Polymer 42 (2001) 4501–4507.
[24] B. Lepoittevin, M. Devalckenaere, N. Pantoustier, M. Alexandre, D. Kubies, C. Calberg, et al., Poly(epsilon-caprolactone)/clay nanocomposites prepared by melt intercalation: mechanical, thermal and rheological properties, Polymer 43 (2002) 4017–4023.
[25] M. Alexandre, P. Dubois, Polymer-layered silicate nanocomposites: preparation, properties and uses of a new class of materials, Mater. Sci. Eng. R. Rep. 28 (2000) 1–63.
[26] T.D. Fornes, P.J. Yoon, H. Keskkula, D.R. Paul, Nylon 6 nanocomposites: the effect of matrix molecular weight, Polymer 42 (2001) 9929–9940.
[27] S.F. Wang, Y. Hu, L. Song, Z.Z. Wang, Z.Y. Chen, W.C. Fan, Preparation and thermal properties of ABS/montmorillonite nanocomposite, Polym. Degrad. Stab. 77 (2002) 423–426.
[28] J.M. Yeh, C.L. Chen, C.C. Huang, F.C. Chang, S.C. Chen, P.L. Su, et al., Effect of organoclay on the thermal stability, mechanical strength, and surface wettability of injection-molded ABS-clay nanocomposite materials prepared by melt intercalation, J. Appl. Polym. Sci. 99 (2006) 1576–1582.
[29] S. Kumar, M. Hofmann, B. Steinmann, E.J. Foster, C. Weder, Reinforcement of stereolithographic resins for rapid prototyping with cellulose nanocrystals, ACS Appl. Mater. Interfaces 4 (2012) 5399–5407.
[30] M. Gurr, D. Hofmann, M. Ehm, Y. Thomann, R. Kubler, R. Mulhaupt, Acrylic nanocomposite resins for use in stereolithography and structural light modulation based rapid prototyping and rapid manufacturing technologies, Adv. Funct. Mater. 18 (2008) 2390–2397.
[31] M. Wozniak, Y. de Hazan, T. Graule, D. Kata, Rheology of UV curable colloidal silica dispersions for rapid prototyping applications, J. Eur. Ceram. Soc. 31 (2011) 2221–2229.
[32] M. Gurr, Y. Thomann, M. Nedelcu, R. Kubler, L. Konczol, R. Mulhaupt, Novel acrylic nanocomposites containing in-situ formed calcium phosphate/layered silicate hybrid nanoparticles for photochemical rapid prototyping, rapid tooling and rapid manufacturing processes, Polymer 51 (2010) 5058–5070.
[33] R.H.A. Haq, M.S. Wahab, Jaimi NI, Fabrication process of polymer nano-composite filament for fused deposition modeling, in: Ismail AE, Nor NHM, Ali MFM, R. Ahmad, I. Masood, Tobi ALM, et al., (Eds.), 4th Mechanical and Manufacturing Engineering, Pts 1 and 2. Trans Tech Publications Ltd, Stafa-Zurich 2014, pp. 8–12.
[34] T. Lan, P.D. Kaviratna, T.J. Pinnavaia, Mechanism of clay tactoid exfoliation in epoxy-clay nanocomposites, Chem. Mater. 7 (1995) 2144–2150.
[35] T. Lan, T.J. Pinnavaia, Clay-reinforced epoxy nanocomposites, Chem. Mater. 6 (1994) 2216–2219.
[36] J.N. Gavgani, A.F. Jolfaei, F. Hakkak, F. Goharpey, Rheological, morphological and thermal properties of pickering-like EVA/organoclay nanocomposites, J. Polym. Res. 22 (2015) 17.
[37] S.K. Lim, E.P. Hong, Y.H. Song, B.J. Park, H.J. Choi, I.J. Chin, Preparation and interaction characteristics of exfoliated ABS/organoclay nanocomposite, Polym. Eng. Sci. 50 (2010) 504–512.
[38] M.I. Triantou, P.A. Tarantili, Studies on morphology and thermomechanical performance of ABS/PC/organoclay hybrids, Polym. Compos. 35 (2014) 1395–1407.
[39] I. Gonzalez, J.I. Eguiazabal, J. Nazabal, Rubber-toughened polyamide 6/clay nanocomposites, Compos. Sci. Technol. 66 (2006) 1833–1843.
[40] H.L. Tekinalp, V. Kunc, G.M. Velez-Garcia, C.E. Duty, L.J. Love, A.K. Naskar, et al., Highly oriented carbon fiber-polymer composites via additive manufacturing, Compos. Sci. Technol. 105 (2014) 144–150.
[41] T.Y. Tsai, C.H. Kuo, W.C. Chen, C.H. Hsu, C.H. Chung, Reducing the print-through phenomenon and increasing the curing degree of UP/ST/organo-montmorillonite nanocomposites, Appl. Clay Sci. 49 (2010) 224–228.